

## Diagrammatic analysis of some contributions to the $\Delta I = 1/2$ rule

Mark B. Wise

*Stanford Linear Accelerator Center, Stanford University, Stanford, California 94305*

Edward Witten

*Department of Physics, Harvard University, Cambridge, Massachusetts 02138*

(Received 23 April 1979)

Higher-order gluon corrections to a particular mechanism for the  $\Delta I = 1/2$  rule are computed using quantum chromodynamics. It is found that due to gauge invariance these corrections leave the form of the lowest-order result essentially unchanged.

### I. INTRODUCTION

The weak decays of strange hadrons are conveniently grouped into three general categories: leptonic, semileptonic, and nonleptonic. While the leptonic and semileptonic decays have been fairly well understood for many years, only recently has serious progress been made towards the understanding of nonleptonic decays.

It is well known that experimentally the nonleptonic decays of strange hadrons which proceed through the  $\Delta I = \frac{1}{2}$  part of the effective weak Hamiltonian are enhanced by roughly a factor of 20 (in amplitude) over those decays which go via the  $\Delta I = \frac{3}{2}$  part of the effective weak Hamiltonian. This is called the  $\Delta I = \frac{1}{2}$  rule. It had been hoped that strong-interaction effects at short distances would sufficiently enhance the  $\Delta I = \frac{1}{2}$  portion of the usual current-current nonleptonic weak Hamiltonian to explain the  $\Delta I = \frac{1}{2}$  rule.<sup>1</sup> However, detailed calculations using quantum chromodynamics (QCD) do not lead to a large enough enhancement.<sup>2</sup>

It has been claimed<sup>3</sup> that the answer lies in the amplitude shown in Fig. 1, sometimes called a "penguin" diagram. Since the gluon ( $g$ ) carries no isospin, this amplitude is pure  $\Delta I = \frac{1}{2}$ . At first glance the penguin diagram appears to give a small contribution to the effective weak Hamiltonian, but its chiral structure leads to a very large contribution to strange-particle decay amplitudes involving pions when its matrix elements are evaluated by saturating the matrix element of a product of quark bilinears with the vacuum intermediate state. Analysis<sup>3-6</sup> of both strange meson and baryon decays supports the hypothesis that both the magnitude of the decay amplitudes and the  $\Delta I = \frac{1}{2}$  rule are understandable on this basis.

Calculation of Fig. 1 reveals that (in the approximation of regarding the  $W$ -boson and charm-quark masses as very heavy) the loop integral gives a factor of  $k^2$  which cancels the pole in the

gluon propagator. As a result Fig. 1 can be described, perhaps surprisingly, in terms of a local four-quark operator in the effective Hamiltonian for nonleptonic weak decays.

It is natural to wonder whether this local four-fermion structure is an artifact of the lowest-order calculation or will persist to higher orders. For example, Fig. 2(a) might appear to be a diagram showing that the local four-fermion result is indeed an artifact of the lowest-order calculation. In Fig. 2(a) the factor of  $k^2$  from the upper loop integration cancels the gluon propagator when the masses of the strange and down quarks are zero. This, however, does not lead to a local four-fermion structure, but instead to a structure of the type shown schematically in Fig. 2(b).

Another class of diagrams that might seem to show that the local four-fermion result of Fig. 1 is an artifact is shown in Fig. 3. Again, the diagrams of this type do not admit an interpretation in terms of a local four-fermion structure. Moreover, they are no smaller than the lowest-order penguin diagram even in the limit of large charm-quark and  $W$ -boson masses. The diagrams of Fig. 3 would, taken by themselves, ruin the lowest-order local four-fermion result.

The purpose of this paper is to show, by explicit calculation, that a cancellation of soft-gluon effects occurs between the diagrams of Figs. 2 and 3 and to show how similar cancellations occur between other diagrams so that in general the

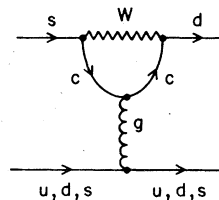


FIG. 1. "Penguin" diagram contributing to nonleptonic weak decays.

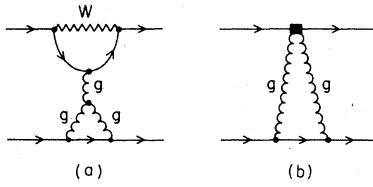


FIG. 2. (a) A two-loop penguin-type diagram contributing to nonleptonic weak decays. (b) Symbolic representation of (a) illustrating the cancellation of a gluon propagator by the upper loop integration.

local four-fermion structure of the effective weak Hamiltonian density is not destroyed.

This cancellation, which might seem surprising from a strictly diagrammatic point of view, actually has a simple and fairly well-established field-theoretic interpretation.<sup>3,4,7-9</sup> To leading order in the heavy masses the sum of all diagrams of the penguin type (with arbitrary gluon insertions) must be equal to a sum of matrix elements of local, gauge-invariant operators times Wilson coefficients.<sup>1</sup> Apart from four-fermion operators, one might expect the operator  $\bar{d} \gamma_\mu (1 - \gamma_5) T^a s (D_\nu F^{\nu\mu})^a$  to appear in the expansion. [Here  $D_\nu F^{\nu\mu} \equiv (D_\nu F^{\nu\mu})^a T^a$  denotes the covariant derivative of the gluon field strength tensor.] Other operators have the wrong dimension, chirality or flavor quantum numbers. But by the equations of motion for QCD this operator is itself a four-fermion operator. Thus the local four-fermion structure of the lowest-order penguin diagram is preserved in the sense that the sum of all penguin-type diagrams equals a sum of Wilson coefficients (which will be modified from their lowest-order values) times matrix elements of local four-fermion operators.

The basic result has already been stated in Refs. 3 and 4. The purpose of this paper is to show, in a diagrammatic language, how the higher-order diagrams manage to preserve the basic structure of the lowest-order result. In the next section, the details of the calculations are outlined. Some comments and the conclusions are stated in Sec. III.

## II. CALCULATIONS

In the absence of strong interactions the weak interactions induce a strange-quark-to-down-

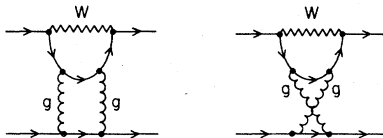


FIG. 3. Two-loop penguin-type diagrams which are not the matrix elements of a local four-fermion operator.

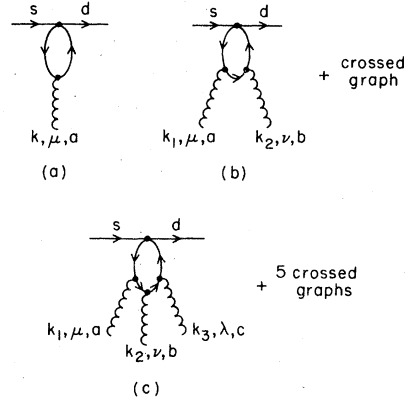


FIG. 4. One-particle-irreducible diagrams contributing to the transition  $s \rightarrow d + (\text{gluons})$  at the one-loop level.

quark transition  $s \rightarrow d$  in the mass matrix which can be absorbed into quark wave-function renormalization if the strange and down quarks are on the mass shell.<sup>10</sup> When the gluon field is present, strangeness-changing transitions such as  $s \rightarrow d + (\text{gluons})$  exist which cannot be absorbed into a redefinition of the fermion fields.

Consider first the contribution of the one-particle irreducible diagram in Fig. 4(a) to the effective weak Hamiltonian. In Fig. 4(a) the cycloidlike line represents the gluon field  $A_\mu^a$ . The  $W$ -boson propagator has been replaced by a Fermi coupling which gives the leading contribution of an expansion in powers of  $1/M_W^2$ . In momentum space Fig. 4(a) gives rise to an effective vertex  $E_1^a(p; k)_\mu$ , where<sup>11</sup>

$$E_1^a(p; k)_\mu = 2\bar{d}_L(p-k) I_\mu^a(k) s_L(p) \quad (1a)$$

and

$$I_\mu^a(k) = \frac{2G}{\sqrt{2}} \int \frac{d^4q}{(2\pi)^4} \gamma^\alpha i \frac{\not{q} - \not{k} + m}{(q-k)^2 - m^2 + i0} \times ig T^a \gamma_\mu i \frac{\not{q} + m}{q^2 - m^2 + i0} \gamma_\alpha. \quad (1b)$$

The SU(3) color matrices  $T^a$ ,  $a \in \{1, 2, \dots, 8\}$ , satisfy the commutation relations

$$[T^a, T^b] = if^{abc} T^c \quad (2a)$$

and the normalization condition

$$\text{Tr}(T^a T^b) = \frac{\delta^{ab}}{2}. \quad (2b)$$

When calculating  $I_\mu^a(k)$  only terms which contribute to leading order in the heavy quark mass  $m$  are kept and  $k^2$  is treated as small compared with  $m^2$ . That is, we work in the soft-gluon and large-quark-mass limit. Since the "infinite" part is independent of the mass of the quark and will cancel by the Glashow-Iliopoulos-Maiani (GIM) mechanism<sup>12</sup> when another quark is added to the

loop of Fig. 4(a), the resulting expression for  $I_\mu^a(k)$  is finite and has the form<sup>3,10</sup>

$$I_\mu^a(k) = \frac{G}{\sqrt{2}} \frac{g}{12\pi^2} \ln\left(\frac{m^2}{\mu^2}\right) T^a(k^2 \gamma_\mu - k_\mu \not{k}). \quad (3)$$

The dependence of the logarithm in Eq. (3) on the renormalization point mass  $\mu$  will cancel by the GIM mechanism, but it is retained at this stage so that the argument of the logarithm appears dimensionless. In the four-quark model, for example, the case of physical interest has a charm quark in the loop. However, a diagram such as Fig. 4(a) with an up quark in the loop arises from the matrix elements of the usual current-current term in the effective Hamiltonian. If the charm quark is treated as heavy, then to leading order in the heavy charm quark mass  $m$  the up quark does not contribute except to cancel the infinite parts and replace  $\mu$  by a typical hadronic mass. This last point is somewhat arbitrary since in the limit where  $m$  is very heavy  $\ln(m^2/\mu^2)$  is approximately independent of  $\mu$ .

Transforming to coordinate space, by the substitution  $k_\mu \rightarrow -i\partial_\mu$ , Fig. 4(a) is represented by the operator

$$\begin{aligned} \mathfrak{C}_1(x) = & -\frac{G}{\sqrt{2}} \frac{g}{12\pi^2} \ln\left(\frac{m^2}{\mu^2}\right) 2\bar{d}_L(x) \gamma_\mu T^a s_L(x) \\ & \times (g^{\mu\nu} \partial^2 - \partial^\mu \partial^\nu) A_\nu^a(x) + \text{H.c.} \end{aligned} \quad (4)$$

$$I_{\mu\nu}^{ab}(k_1, k_2) = -\frac{iG}{\sqrt{2}} \frac{g^2}{12\pi^2} \ln\left(\frac{m^2}{\mu^2}\right) T^c f^{cab} [(2k_2 + k_1)_\mu \gamma_\nu - (2k_1 + k_2)_\nu \gamma_\mu + (k_1 - k_2) g_{\mu\nu}]. \quad (6)$$

The "infinite" part is omitted since it is independent of the quark mass  $m$  and will cancel by the GIM mechanism. In coordinate space, Fig. 4(b) is represented by the operator

$$\mathfrak{C}_2(x) = -\frac{G}{\sqrt{2}} \frac{g^2}{12\pi^2} \ln\left(\frac{m^2}{\mu^2}\right) 2\bar{d}_L(x) \gamma^\mu T^c s_L(x) f^{cab} [2A_\nu^a(x) \partial^\nu A_\mu^b(x) + A_\mu^b(x) \partial^\nu A_\nu^a(x) + A^{\nu b}(x) \partial_\mu A_\nu^a(x)] + \text{H.c.} \quad (7)$$

in the effective weak Hamiltonian density. If Fig. 4(b) as a subdiagram of Fig. 3 could be replaced by the effective vertex in Eqs. (5) and (6) then Fig. 3 would be included in the matrix elements of  $\mathfrak{C}_2$  evaluated at the one-loop level. There would then be a complete cancellation<sup>15</sup> between the diagrams in Fig. 3 and the diagram in Fig. 2(a), which is included in the matrix elements of  $\mathfrak{C}_1$  evaluated at the one-loop level. However, such a substitution is only valid if the gluon momenta  $k_1$  and  $k_2$  can be considered as small compared to the heavy quark mass. If one differentiates the diagrams in Fig. 3 with respect to an external momentum, their ultraviolet convergence is improved enough for the substitution of the effective vertex in Eq. (5).<sup>16</sup> It follows that the sum of diagrams in Figs. 2(a) and 3 is a constant independent of external momenta and thus is proportional to

in the effective weak Hamiltonian density. Note that Eq. (4) does not contain the heavy quark field. In general we want to derive an effective Hamiltonian density independent of the heavy quark field.<sup>13,14</sup> Of course, matrix elements of this Hamiltonian must be evaluated to all orders in the theory of strong interactions.

The matrix elements of the operator in Eq. (4) reproduce the amplitude for the lowest-order penguin diagram in Fig. 1 and the amplitude for the diagram in Fig. 2.

Next consider the case where two gluon fields are attached to the quark loop as shown in Fig. 4(b). In momentum space, Fig. 4(b) gives rise to an effective vertex  $E_2^{ab}(p; k_1, k_2)_{\mu\nu}$  which has the form

$$E_2^{ab}(p; k_1, k_2)_{\mu\nu} = 2\bar{d}_L(p - k_1 - k_2) I_{\mu\nu}^{ab}(k_1, k_2) s_L(p). \quad (5)$$

The calculation of  $I_{\mu\nu}^{ab}(k_1, k_2)$  is simplified by noting that only logarithmically divergent integrals have the potential to give rise to a logarithmic enhancement in the heavy-quark mass  $m$ . Explicit calculation to leading order in the heavy-quark mass  $m$  reveals that in the soft-gluon and large-quark-mass limit where  $k_1^2$ ,  $k_2^2$  and  $k_1 \cdot k_2$  are treated as small compared with  $m^2$

the tree approximation for the matrix elements of a local four-quark operator. Thus the sum of the two-loop diagrams in Figs. 2(a) and 3 just gives a higher-order (i.e., order  $g^4$ ) contribution to the Wilson coefficients of local four-fermion operators and does not change the basic form of the lowest-order result due to the one-loop diagram in Fig. 1. Note that the corrections to the Wilson coefficients given by the diagrams in Figs. 2(a) and 3 depend on the choice of renormalization scheme. We use a mass-independent renormalization scheme.<sup>17,18</sup>

At the two-loop level we also encounter diagrams such as Fig. 5 which give higher-order contributions both to matrix elements of  $\mathfrak{C}_1$  and to Wilson coefficients of local four-quark operators in the effective Hamiltonian for nonleptonic weak decays. If Fig. 4(a) as a subdiagram of Fig. 5 could

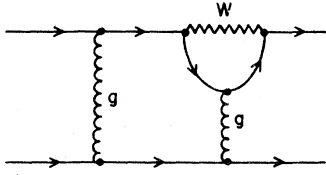


FIG. 5. Example of a two-loop diagram that gives a higher-order contribution to both the matrix elements of  $\mathcal{H}_1$  and to the Wilson coefficients of local four-quark operators in the effective Hamiltonian.

be replaced by the effective vertex in Eqs. (1a) and (3), then Fig. 5 would simply be a higher-order contribution to the matrix elements. However, the ultraviolet convergence is not good enough for this simple substitution. Differentiating with respect to an external momentum reveals that Fig. 5 differs from a higher-order contribu-

$$I_{\mu\nu\lambda}^{abc}(k_1, k_2, k_3) = \frac{G}{\sqrt{2}} \frac{g^3}{12\pi^2} \ln\left(\frac{m^2}{\mu^2}\right) T^d [(f^{eab}f^{ecd} - f^{ebc}f^{ead})g_{\lambda\mu}\gamma_\nu - (f^{eab}f^{ecd} + f^{eac}f^{ebd})g_{\lambda\nu}\gamma_\mu + (f^{eac}f^{ebd} + f^{ebc}f^{ead})g_{\mu\nu}\gamma_\lambda], \quad (9)$$

where the "infinite" part which is independent of the quark mass  $m$  has been omitted. Transforming to coordinate space, Fig. 4(c) is represented by the operator

$$\mathcal{H}_3(x) = -\frac{G}{\sqrt{2}} \frac{g^3}{12\pi^2} \ln\left(\frac{m^2}{\mu^2}\right) 2\bar{d}_L(x)\gamma^\mu T^d s_L(x) f^{ebc}f^{ead} [A_\nu^a(x)A^\nu(x)] A_\mu^b(x) + \text{H.c.} \quad (10)$$

in the effective weak Hamiltonian density.

Using these results we see that a cancellation<sup>15</sup> at the three-loop level occurs which is similar to the one between the two-loop diagrams in Fig. 2(a) and 3. The three-loop diagrams in Fig. 6 cancel up to terms independent of external momenta, which are proportional to the tree approximation for the matrix elements of local four-quark operators. Thus, taken together, the diagrams in Fig. 6 give an order- $g^6$  contribution to the Wilson coefficients of local four-fermion operators, preserving the basic form of the lowest-order result.

In the large-quark-mass and soft-gluon limit terms with more than three gluon fields attached to the quark loop do not contribute to the transition  $s \rightarrow d + (\text{gluons})$  at the one-loop level since such graphs are finite without the GIM mechanism and are incapable of producing a logarithmic en-

hancement in the heavy-quark mass. Thus, apart from Cabibbo-type angles and terms that will cancel by the GIM mechanism, diagrams contributing to the process  $s \rightarrow d + (\text{gluons})$  with a heavy quark in the loop give rise, at the one-loop level, to an effective weak Hamiltonian density

$$E_3^{abc}(p; k_1, k_2, k_3)_{\mu\nu\lambda} = 2\bar{d}_L(p - k_1 - k_2 - k_3) \times I_{\mu\nu\lambda}^{abc}(k_1, k_2, k_3) s_L(p) \quad (8)$$

and direct calculation in the large-quark-mass and soft-gluon limit gives

hancement in the heavy-quark mass. Thus, apart from Cabibbo-type angles and terms that will cancel by the GIM mechanism, diagrams contributing to the process  $s \rightarrow d + (\text{gluons})$  with a heavy quark in the loop give rise, at the one-loop level, to an effective weak Hamiltonian density

$$\begin{aligned} \mathcal{H}^{\text{penguin}}(x) &= \mathcal{H}_1(x) + \mathcal{H}_2(x) + \mathcal{H}_3(x) \\ &= -\frac{G}{\sqrt{2}} \frac{g}{12\pi^2} \ln\left(\frac{m^2}{\mu^2}\right) 2\bar{d}_L(x)\gamma^\nu T^a s_L(x) \\ &\quad \times [D^\mu F_{\mu\nu}(x)]^a + \text{H.c.} \end{aligned} \quad (11)$$

### III. COMMENTS AND CONCLUSIONS

Using the equations of motion for QCD,

$$(D^\mu F_{\mu\nu})^a = J_\nu^a \equiv g(\bar{u}\gamma_\nu T^a u + \bar{d}\gamma_\nu T^a d + \bar{s}\gamma_\nu T^a s), \quad (12)$$

the effective weak Hamiltonian density in Eq. (11) becomes the local four-quark operator

$$\mathcal{H}^{\text{penguin}}(x) = -\frac{G}{\sqrt{2}} \frac{g^2}{12\pi^2} \ln\left(\frac{m^2}{\mu^2}\right) 2\bar{d}_L(x)\gamma^\nu T^a s_L(x) [\bar{u}(x)\gamma_\nu T^a u(x) + \bar{d}(x)\gamma_\nu T^a d(x) + \bar{s}(x)\gamma_\nu T^a s(x)] + \text{H.c.} \quad (13)$$

This is essentially the same result as a lowest order in perturbation theory calculation of Fig. 1 gives but the derivation is more satisfactory since higher-order QCD effects have been taken into

account. Of course, using gauge invariance and the result of Eq. (4) one can immediately conclude that the effective weak Hamiltonian density must contain Eq. (13). What we have shown, by explicit

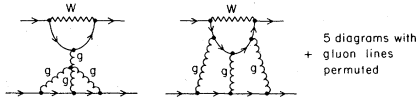


FIG. 6. Three-loop penguin-type diagrams which together are proportional to the tree approximation for the matrix elements of a local four-fermion operator.

calculation, is how the various pieces combine to give a local gauge-invariant contribution and that in the large quark mass limit no other gauge-invariant contributions occur. Other possible gauge-invariant contributions are either higher order in  $1/M_W^2$  or lower order in  $m^2$ . For example, if the strange and down quark masses are not taken to be zero, diagrams at the one-loop level also give rise to a transition color magnetic moment term. However, its contribution<sup>10</sup> to the effective weak Hamiltonian density is multiplied by a factor  $m^2/M_W^2$  so it is suppressed by an extra power of  $1/M_W^2$  (apart from logarithms) provided  $M_W^2 \gg m^2$ , as we have implicitly assumed by the order in which the large- $M_W$  and large- $m$  limits were taken.

We have also shown how diagrams with more

than one loop, such as those in Figs. 2, 3, and 6, combine together with soft-gluon effects canceling because of gauge invariance and hard-gluon effects giving higher-order contributions to the Wilson coefficients of local four-fermion operators. Of course, one also encounters from diagrams beyond the one-loop level (e.g., from Fig. 5) corrections to the matrix elements of the local four-fermion operators occurring in the effective Hamiltonian for nonleptonic weak decays. What is preserved is the fact that the sum of all penguin-type diagrams (with arbitrary gluon insertions) can be represented by a sum of Wilson coefficients times matrix elements of local four-fermion operators.

#### ACKNOWLEDGMENTS

We are grateful to F. Gilman for useful discussions. One of us (M.B.W.) also thanks L. Abbott and S. Brodsky for some helpful suggestions. This work was supported in part by the U. S. Department of Energy under Contract No. EY-76-C-03-0515. M.B.W. also received financial support from the National Research Council of Canada and Imperial Oil Limited.

<sup>1</sup>K. G. Wilson, Phys. Rev. **179**, 1499 (1969).

<sup>2</sup>M. K. Gaillard and B. W. Lee, Phys. Rev. Lett. **33**, 108 (1974); G. Altarelli and L. Maiani, Phys. Lett. **52B**, 351 (1974).

<sup>3</sup>A. I. Vainshtein *et al.*, Zh. Eksp. Teor. Fiz. Pis'ma Red. **22**, 123 (1975); [JETP Lett. **22**, 55 (1975)]; M. A. Shifman *et al.*, Nucl. Phys. **B120**, 316 (1977).

<sup>4</sup>M. A. Shifman *et al.*, ITEP Reports Nos. ITEP-63, ITEP-64, 1976 (unpublished).

<sup>5</sup>M. K. Gaillard, *Weak Interactions—Present and Future*, Proceedings of the SLAC Institute on Particle Physics, 1978, edited by M. C. Zipf (SLAC, Stanford, 1978).

<sup>6</sup>J. Finjord, Phys. Lett. **76B**, 116 (1978).

<sup>7</sup>E. Witten, Nucl. Phys. **B122**, 109 (1977).

<sup>8</sup>A. I. Vainshtein *et al.*, Phys. Lett. **60B**, 71 (1975); Yad. Fiz. **23**, 1024 (1976) [Sov. J. Nucl. Phys. **23**, 540 (1976)]; A. I. Vainshtein *et al.*, Zh. Eksp. Teor. Fiz. Pis'ma Red. **23**, 656 (1976) [JETP Lett. **23**, 602 (1976)]; Zh. Eksp. Teor. Fiz. **72**, 1275 (1977) [Sov. Phys.—JETP **45**, 670 (1977)].

<sup>9</sup>V. A. Novikov *et al.*, Phys. Rev. D **16**, 223 (1977).

<sup>10</sup>M. K. Gaillard and B. W. Lee, Phys. Rev. D **10**, 897 (1974).

<sup>11</sup>In Eq. (1a)  $d_L$  and  $s_L$  denote left-handed down and strange quarks. In Eq. [1(b)]  $G$  is the Fermi weak

coupling constant,  $m$  is the mass of the quark in the loop of diagrams in Fig. 4 and  $g$  is the strong coupling.

<sup>12</sup>S. L. Glashow, J. Iliopoulos, and L. Maiani, Phys. Rev. D **2**, 1285 (1970).

<sup>13</sup>T. Appelquist and J. Carrazzone, Phys. Rev. D **11**, 2856 (1975).

<sup>14</sup>E. Witten, Nucl. Phys. **B120**, 387 (1977).

<sup>15</sup>We assume that the masses of the external strange and down quarks are zero. While making this assumption is not crucial, it simplifies the details of how particular cancellations take place and ensures that a transition color magnetic moment term does not arise in the effective Hamiltonian for nonleptonic weak decays.

<sup>16</sup>To see that a simple replacement of the subdiagram Fig. 4 (b), of the diagrams in Fig. 3, by the effective vertex in Eqs. (5) and (6) is not correct, we note by naive power counting that such a substitution would introduce an ultraviolet divergence. Differentiating with respect to an external momentum removes this ultraviolet divergence, so that the loop integral is then dominated by gluon momenta  $k_1$  and  $k_2$  of the same order as the external momenta. A detailed discussion of this technique can be found in Ref. 7.

<sup>17</sup>S. Weinberg, Phys. Rev. D **8**, 3497 (1973).

<sup>18</sup>G. 't Hooft, Nucl. Phys. **B61**, 455 (1973).